Journal of Solid State Chemistry 250 (2017) 100–106

Contents lists available at ScienceDirect

Journal of Solid State Chemistry

journal homepage: www.elsevier.com/locate/jssc

Magnetic interactions in praseodymium ruthenate Pr_3RuO_7 with fluorite-related structure

Masaki Inabayashi, Yoshihiro Doi, Makoto Wakeshima, Yukio Hinatsu*

Division of Chemistry, Graduate School of Science, Hokkaido University, Sapporo 060-0810, Japan

ARTICLE INFO

Keywords:
Magnetic properties
Praseodymium
Ruthenium
Oxides
Antiferromagnetic transition

ABSTRACT

Solid solutions $Pr_3(Ru_{1-x}Ta_x)O_7$ ($0 \le x \le 1.0$) and $(Pr_{1-x}Y_x)_3RuO_7$ ($0 \le x \le 0.7$) were obtained as a single phase compound. They crystallize in an orthorhombic superstructure derived from that of the cubic fluorite with space group *Cmcm*. The results of the Rietveld analysis for X-ray diffraction profiles of $Pr_3(Ru_{1-x}Ta_x)O_7$ showed that Ru and Ta atoms are randomly situated at the six-coordinate 4*b* site. For $(Pr_{1-x}Y_x)_3RuO_7$, with increasing the concentration of Y ions (*x* value), the smaller Y ions occupy selectively the seven-coordinate 8*g* site rather than the eight-coordinate 4*a* site.

Through magnetic susceptibility measurements for $Pr_3(Ru_{1-x}Ta_x)O_7$, the antiferromagnetic transition temperatures decrease linearly with increasing *x* value, and at $x=0.75$ no magnetic ordering was found down to 1.8 K, indicating the magnetic interaction is not one-dimensional, but three-dimensional. On the other hand, the antiferromagnetic transition temperature for $(Pr_{1-x}Y_x)_3RuO_7$ decreases with increasing *x* value, but above $x \ge 0.50$ it becomes constant (~12 K). This result indicates that Pr^{3+} ions at the seven-coordinate site greatly contribute to the antiferromagnetic interactions observed in $(Pr_{1-x}Y_x)_3RuO_7$.

Density functional calculations of Pr_3RuO_7 demonstrate that the electronic structure gives insulating character and that oxygen 2p orbitals hybridize strongly with Ru 4d orbitals in the valence band (VB). Near the top of VB, the Pr 4 f orbitals at the seven-coordinated site also show a weak hybridization with the O(1) 2p orbitals. The Ru-O(1)-Pr superexchange pathway take part in three-dimensional magnetic interaction and play an important role in an enhancement of long-range magnetic ordering.

1. Introduction

Magnetic properties of compounds containing both rare earth and transition metal have attracted a great deal of interest, because they often show anomalous magnetic behavior due to interactions of unpaired *f* electrons and *d* electrons.

Among them, compounds of composition Ln_3MO_7, where *Ln* is a rare earth and *M* is the 4*d* or 5*d* transition metal, have been investigated by many researchers. They have a defect-fluorite structure. The relationship to the fluorite structure is as follows. The fluorite unit cell for oxides has the composition $M^{4+}{}_4O_8$. If the four tetravalent metal ions are replaced by three trivalent ions (*Ln*) and one pentavalent ion (*M*), one oxide vacancy is formed per fluorite cell. Due to significant differences in radii between the Ln^{3+} and M^{5+} ions, cation ordering occurs on the metal sites and the oxide-vacancy orders on the anion sites. The M^{5+} ion is coordinated with six oxygen ions, forming an MO_6 octahedron. These octahedra share corners forming one-dimensional chains which are oriented along the *c*-axis.

Many studies have been performed, due to this unique crystal structure and possible related magnetic properties for Ln_3MO_7 compounds (*M*=Mo [1–3], Ru [4–17], Re [18–21], Os [13,22–24], and Ir [25–28]), especially for the magnetic properties of compounds containing Ru^{5+} ion at the *M*-site because of its largest possible spin ($S=3/2$) among the 4*d* and 5*d* transition metals. Among many Ln_3MO_7 compounds, we focus our attention on the magnetic properties of Pr_3RuO_7. Magnetic susceptibility and specific heat measurements show that Pr_3RuO_7 orders magnetically at 55 K [8]. This ordering temperature is the highest compared with those for other Ln_3MO_7 compounds.

In order to clarify why Pr_3RuO_7 shows such high magnetic transition temperature, we prepared two types of solid solutions in which magnetic ions (Ru^{5+} and Pr^{3+}) are replaced by diamagnetic ions, i.e., $Pr_3(Ru_{1-x}Ta_x)O_7$ and $(Pr_{1-x}Y_x)_3RuO_7$. Through X-ray diffraction measurements, their structures were determined, and magnetic susceptibility measurements were performed from 1.8 to 400 K to study their magnetic properties. We also performed calculations of the electronic structure and the density of states (DOS) for Pr_3RuO_7.

* Corresponding author.
E-mail address: hinatsu@sci.hokudai.ac.jp (Y. Hinatsu).

http://dx.doi.org/10.1016/j.jssc.2017.03.025
Received 24 February 2017; Received in revised form 28 March 2017; Accepted 30 March 2017
Available online 31 March 2017

2. Experimental

2.1. Sample preparation

2.1.1. $Pr_3(Ru_{1-x}Ta_x)O_7$

Solid solutions $Pr_3(Ru_{1-x}Ta_x)O_7$ (x=0, 0.1, 0.2. –, 0.9, 1.0) were prepared by the conventional solid state reactions. As starting materials, praseodymium oxide Pr_6O_{11}, ruthenium dioxide RuO_2, and tantalum oxide Ta_2O_5 were used. They were weighed in an appropriate metal ratio and the mixtures were ground in an agate mortar. The mixtures were pressed into pellets and then heated in air at 1300 °C for 12 h. After cooling to room temperature, the pellets were crushed, re-pressed into pellets, and reheated in the same conditions. These procedures were repeated four times with several intermediate grindings.

2.1.2. $(Pr_{1-x}Y_x)_3RuO_7$

Pr_6O_{11}, Y_2O_3 and RuO_2 were used as starting materials. After weighing these materials, they were dissolved in heated nitric acid. RuO_2 does not dissolve and remains as powders. Then, citric acid and ethylene glycol were added to this solution with a molar ratio of 5:1 against the $(Pr_{1-x}Y_x)_3RuO_7$. The precipitates were percolated and heated in air at 675 °C for 12 h. After cooling to room temperature, the mixtures were ground in an agate mortar. The mixtures were pressed into pellets and then heated in air at 1300 °C for 12 h.

2.2. X-ray Diffraction analysis

Powder X-ray diffraction profiles were measured using a Rigaku Multi-Flex diffractometer with Cu-Kα radiation (λ=1.5406 Å) equipped with a curved graphite monochromator. The data were collected by step-scanning in the angle range of 10°≤2θ≤120° at a 2θ step-size of 0.02°.

The X-ray diffraction data were analyzed by the Rietveld technique, using the programs RIETAN-FP [29], and the crystal structure was drawn by using the VESTA program [30].

2.3. Magnetic susceptibility measurements

The temperature-dependence of the magnetic susceptibility was measured in an applied field of 0.1 T over the temperature range of 1.8 K≤T≤300 K, using a SQUID magnetometer (Quantum Design, MPMS5S). The susceptibility measurements were performed under both zero-field-cooled (ZFC) and field-cooled (FC) conditions. The former was measured upon heating the sample to 300 K under the applied magnetic field of 0.1 T after zero-field cooling to 1.8 K. The latter was measured upon cooling the sample from 300 to 1.8 K at 0.1 T.

2.4. DFT calculation

Calculations of the electronic structure and the density of states (DOS) were performed using the WIEN2k program package [31]. This program employs the full–potential linearized augmented plane wave +local orbitals (FP–LAPW+lo) method based on density functional theory (DFT). We used the generalized gradient approximation (GGA)+Hubbard U parameter for the Ru 4d and the Pr 4f electrons with spin-orbit coupling (SOC). In the calculations, the convergence parameter was set to be $R_{MT}k_{max}$=7.0, and the muffin–tin (MT) spheres are R_{MT}(Pr) =2.20 bohr, R_{MT}(Ru)=1.96 bohr, and R_{MT}(O)=1.69 bohr. We used 10×10×8 meshes with 120 k points in the first Brillouin zone (B.Z.). The U parameters of Ru 4d and Pr 4f orbitals are set to be 3.0 eV and 4.0 eV, respectively.

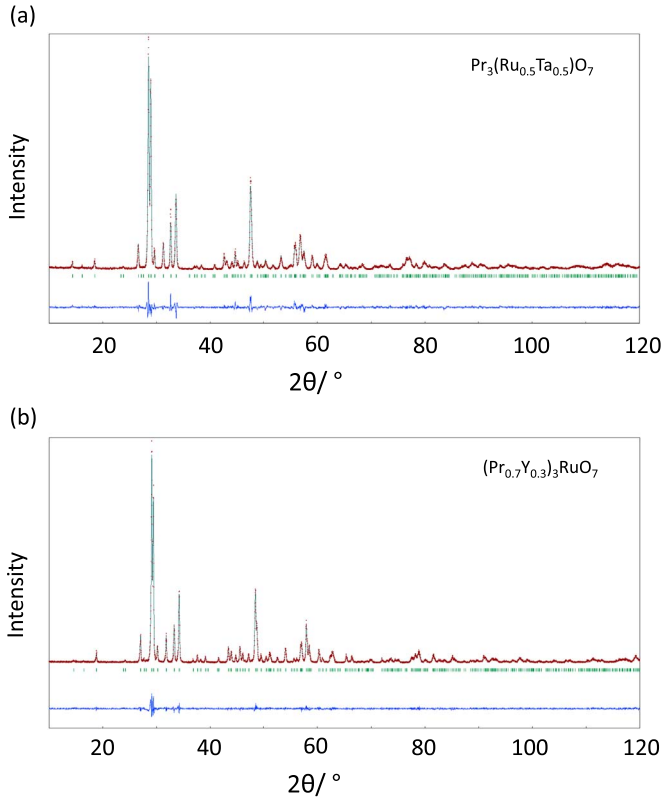

Fig. 1. Powder x-ray diffraction profiles for (a) $Pr_3(Ru_{0.5}Ta_{0.5})O_7$ and (b) $(Pr_{0.7}Y_{0.3})_3RuO_7$. The calculated and observed profiles are shown on the top solid line and cross markers, respectively. The vertical marks in the middle show positions calculated for Bragg reflections. The lower trace is a plot of the difference between calculated and observed intensities.

3. Results and discussion

3.1. $Pr_3(Ru_{1-x}Ta_x)O_7$

For all $Pr_3(Ru_{1-x}Ta_x)O_7$ (x=0, 0.1, 0.2. –, 0.9, 1.0), single-phase compounds were obtained. Fig. 1(a) shows the X-ray diffraction profile of $Pr_3(Ru_{0.5}Ta_{0.5})O_7$. The diffraction patterns are similar to that for the fluorite structure and all reflections appeared to be consistent with the C-centered conditions, h+k=2n, and h 0 l reflections with odd l are absent. We have analyzed the X-ray diffraction profiles with the space group $Cmcm$, which is the same space group as those for end members Pr_3RuO_7 [8] and Pr_3TaO_7 [32]. All the reflections observed could be successfully indexed. The crystallographic data determined for $Pr_3(Ru_{0.5}Ta_{0.5})O_7$ are listed in Table 1.

Complete solid solutions are formed for $Pr_3(Ru_{1-x}Ta_x)O_7$. The

Table 1
Structural parameters for $Pr_3(Ru_{0.5}Ta_{0.5})O_7$.

Atom	Site	occupancy	x	y	z	B /Å^2
Pr(1)	4a	1.0	0	0	0	0.59(3)
Pr(2)	8g	1.0	0.225(8)	0.303(1)	1/4	0.59
Ru/Ta	4b	0.5/0.5	0	1/2	0	0.13
O(1)	16h	1.0	0.121(7)	0.316(7)	-0.038(8)	1.0
O(2)	8g	1.0	0.135(4)	0.025(8)	1/4	1.0
O(3)	4c	1.0	0	0.439(5)	1/4	1.0

Note. Space group $Cmcm$; a=10.9835(3) Å, b=7.4673(6) Å, c=7.6227(5) Å, V=625.20(3) Å^3, R_{wp}=12.72%, R_B=2.61%, and R_e=9.93%, where $R_{wp} = [\sum_i w_i(y_i - f_i(\mathbf{x}))^2/\sum_i w_i y_i^2]^{1/2}$, $R_B = \sum_K |I_O(\mathbf{h}_K) - I(\mathbf{h}_K)|/\sum_K I_O(\mathbf{h}_K)$, and $R_e = [(N-P)/\sum_i w_i y_i^2]^{1/2}$.